

The photodegradation of Pyrromethene 567 and Pyrromethene 597 by Pyrromethene 546

Nobuaki Tanaka ^a, Wade N. Sisk ^{b,*}

^aDepartment of Environmental Science and Technology, Shinshu University

4-17-1 Wakasato, Nagano, Nagano 380-8553, Japan

^bChemistry Department, University of North Carolina at Charlotte

9201 University City Blvd., Charlotte, NC 28223-0001, USA

Tel: (704) 687-4433, Fax: (704) 687-3151

E-mail: wsisk@email.uncc.edu

Abstract

The photo-destabilizing action of 1,3,5,7,8-pentamethylpyrromethene difluoroborate complex (PM546) on 1,3,5,7,8-pentamethyl-2,6-diethylpyrromethene difluoroborate complex (PM567) and 1,3,5,7,8-pentamethyl-2,6-di-*t*-butylpyrromethene difluoroborate complex (PM597) has been investigated. Acetonitrile solutions of PM567 and PM597 demonstrated accelerated photodegradation upon the addition of PM546; whereas the photodegradation rate of the corresponding *n*-hexane solutions remained invariant with respect to PM546 addition. The enhanced photodegradation rate is explained by electron transfer from PM567 and PM597 to PM546. A PM546 singlet oxygen (¹O₂, O₂ (a¹Δ_g)) quenching rate constant of 3.86 ± 0.18(2σ) × 10⁷ dm³ mol⁻¹ s⁻¹ is obtained from infrared phosphorescence measurements of O₂ (a¹Δ_g → X³Σ_g⁻).

Keywords: singlet oxygen, pyrromethene dyes, photostability, phosphorescence, quenching, electron transfer

1. Introduction

The photostability of organic dyes limits their practical applications to photonics where long lifetime and durability are required. Previous investigations have measured the photostabilities of organic dyes possessing high fluorescence quantum yields such as pyrromethene difluoroborate complexes (PM dyes) and perylene diimides [1-5]. Molecular oxygen O₂ plays an important role in the photodegradation mechanism of dyes and pigments [6,7]. The photobleaching mechanism may depend on oxygen and the nature of the solvent. In the pursuit of higher laser damage thresholds and enhanced durability against photodegradation, a thorough investigation of the effect of additives on the photodegradation mechanism should be undertaken.

Ahmad et al. reported the photostability improvement of PM567/ethanol solutions and polymer dispersed PM567 by the addition of Coumarin 540 (C540) [8]. On the other hand, Jones reported fluorescence quenching of pyrromethene dye acetonitrile solutions by electron acceptors such as methyl viologen or pyromellitic dianhydride via electron transfer [9]. Electron transfer is one of the most fundamental reactions in chemistry and biology. A number of important processes including photosynthesis involve electron transfer. Even in systems where electron transfer is not energetically favorable in the ground state, photoexcitation would induce the reaction.

In this paper we report on the change in photodegradation rates of PM567 and PM597 solutions by PM546 addition following intense 532 nm laser irradiation. To better understand the role of PM546 in the photodegradation of PM567 and PM597, the singlet oxygen quenching rate constant of PM546 has been determined in acetonitrile solution.

2. Experimental

Pyromethenes 546, 567 and 597 were obtained from Exciton Inc. and used as received. Rose Bengal was obtained from Aldrich and used without any further purification. Acetonitrile (HPLC grade) and *n*-hexane (ultimAR grade) were obtained from Aldrich and Mallinckrodt, respectively. The 2nd harmonic of a Q-switched Nd:YAG laser (Continuum Surelite, 8 ns FWHM, 10 Hz) was used as an excitation source.

Photostability experiments were carried out for 1.0×10^{-5} mol dm⁻³ acetonitrile solutions of PM597/PM546 and PM567/PM546 and for 1.0×10^{-5} mol dm⁻³ *n*-hexane solutions of PM597/PM546 with varying PM546 concentration. Photodegradation was monitored by measuring absorption spectra with a Varian Cary 300 Bio uv-vis spectrophotometer following 532 nm irradiation. To accelerate photodegradation a laser fluence of 148.6 mJ cm⁻² pulse⁻¹ was used to irradiate 1.5 ml of the sample solution.

Fluorescence quenching of PM597 by PM546 in acetonitrile was measured using a Jobin Yvon Spex Fluorolog-3 spectrofluorimeter with a front-surface excitation emission geometry.

For singlet oxygen quenching measurements 3.0 ml of 5.6×10^{-5} mol dm⁻³ rose bengal acetonitrile solutions with varying PM546 concentrations were excited at 532 nm. The resulting 1270 nm phosphorescence attributed to O₂ ($a^1\Delta_g \rightarrow X^3\Sigma_g^-$) was detected at right angles to the laser propagation and filtered by three high pass filters (Rolyn OG-5550, 65.1398, 65.1400) and a 1270 nm narrow bandpass filter (Spectrogon Filter N13-1270-010-8). The low laser intensity of 1.6 mJ cm⁻² pulse⁻¹ ensures a linear phosphorescence response. The filtered infrared phosphorescence was imaged onto the active element (0.5 cm × 0.5 cm) of a Judson germanium photodiode (J16D-M204-R05M-60) equipped with a preamplifier (PA-9-44) via a Herasil 1 inch *f*/1 lens. The photodiode output was collected and averaged over 20 laser pulses by a LeCroy

9350 500 MHz digital oscilloscope. The averaged phosphorescence decay profiles were stored on a personal computer. Three phosphorescence profiles were recorded for fresh solutions for each concentration.

Geometry optimizations of the S_0 and T_1 states of the PM dyes were performed using Becke's three-parameter hybrid density functional in combination with the Lee-Yang-Parr correlation functional (B3LYP) and Handy's pure density functional including gradient-corrected correlation (HCTH). All calculations were performed using Gaussian 03W [10].

3. Results and discussion

3.1. Photostability of PM567 and PM597 in solution

Fig. 1 shows a change in absorption spectra of PM597 in acetonitrile upon laser irradiation.

(Fig. 1)

The peaks due to PM597 decrease while absorbance increases and isosbestic points are observed near 300 and 430 nm.

Relative absorbance changes of PM567/acetonitrile, PM597/acetonitrile and PM597/*n*-hexane solutions are compared in Fig. 2.

(Fig. 2)

After 36,000 pump pulses a 34% and 51% decrease in absorbance was observed for acetonitrile solutions of PM567 and PM597, respectively. This degradation rate disparity may be attributed to the difference in the 532 nm absorption coefficients [3]. In contrast with the results in polar acetonitrile, a 14% decrease in PM597 absorbance was observed in *n*-hexane. This is consistent with previous photostability studies [11]. The photostability of pyrromethene dyes in

non-polar solvents exceeds that of the polar solvents. One possible explanation for the higher photodegradation rate in polar solvents is due to the contribution of an oxygen independent mechanism which was postulated to explain the enhanced photodegradation rate of PM567 thin films upon the application of an electric field [12].



Polar solvents would achieve better stabilization of the free ions (Eq. (4)), thus resulting in more reaction products per unit time.

In a recent study of PM597 photodegradation in methanol dye photodegradation was observed to be 2nd order with respect to PM597 concentration in accordance with Eq. (7) [5].

$$\frac{[PM\ 597]_0}{[PM\ 597]} = 1 + [PM\ 597]_0 kt \quad (7)$$

In the present investigation, least-squares fits of acetonitrile and *n*-hexane solutions of PM597 photodegradation to Eq. (7) are shown in Fig. 3.

(Fig. 3)

The linear dependence of PM597/*n*-hexane solutions to Eq. (7) suggests a photodegradation rate that is 2nd order with respect to concentration consistent with PM597/methanol photodegradation [5]. The nonlinear fit of PM597/acetonitrile solutions may be attributed to longer singlet oxygen lifetimes and/or faster ¹O₂ quenching by PM597 in acetonitrile relative to hexane [5,13,14].

Fig. 4 shows the effect of 2.5×10^{-5} mol dm⁻³ PM546 addition on the photostability of 1.0×10^{-5} mol dm⁻³ PM567 and PM597. Addition of PM546 resulted in significantly faster photodegradation of PM567 and 597 in acetonitrile.

(Fig. 4)

On the other hand in *n*-hexane, PM546 addition resulted in a nominal change in the photodegradation rate of PM597 and PM567. There is no significant decrease in absorbance of PM546. Fig. 5 compares the ratios of the absorbance of PM567 and PM597 in acetonitrile after 36,000 laser pulses for several PM546 concentrations, where A_0 and A represent the absorbance in the absence and the presence of PM546 addition after 36,000 laser pulses.

(Fig. 5)

As the concentration of PM546 increases, the ratios A_0/A monotonically increases.

In order to investigate the effect of oxygen, deoxygenated sample solutions were irradiated. Significant improvement in photostability is observed in Fig. 6. Under these conditions photooxidation via oxygen is inoperative, however accelerated photodegradation following PM546 addition occurs for acetonitrile samples under vacuum. Thus, other photodegradation mechanisms need to be considered.

(Figs. 6)

These alternative photodegradation mechanisms may involve the chemical reaction or complex formation between PM546 and PM597. Complex formation and chemical reaction were evaluated by analyzing the emission and absorption spectra. Fluorescence quenching of PM597 by PM546 in acetonitrile is shown in Fig. 7. There is no change in the shape of the fluorescence spectra which suggests no exciplex formation. Absorption spectra even at the highest concentration of PM546 can be reproduced by the sum of the PM597 and PM546 spectra, indicating no ground state complex formation. The bimolecular quenching constant k_q is estimated using the Stern-Volmer equation,

$$I_0/I = 1 + k_q \tau_0 [\text{PM546}] \quad (8)$$

where I_0 and I are the fluorescence intensities in the absence and the presence of the quencher and τ_0 is the fluorescence lifetime of PM597, 4.27 ns [15] in the absence of the quencher. The I_0/I versus [PM546] plot is observed to be linear. Linear regression analysis resulted in a bimolecular quenching constant of $2.6 \times 10^{10} \text{ dm}^3 \text{ mol}^{-1} \text{ s}^{-1}$.

(Fig. 7)

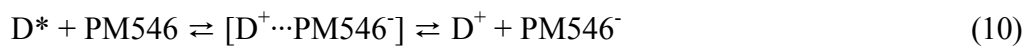
3.2. Effect of PM546 addition

To rationalize the higher PM597 photodegradation rate and PM597 fluorescence quenching upon PM546 addition, additional elementary reactions should be considered in the photodegradation model [5]. Additional processes to consider in PM597 photophysics are: (1) dipole-dipole interaction induced singlet-singlet energy transfer, (2) Dexter triplet-triplet energy transfer, (3) PM546 sensitized singlet oxygen generation and (4) excited state electron transfer from PM dyes to PM546. The singlet-singlet energy transfer mechanism can be ruled out since the S_1 state energy of PM546 is much higher than those of the other PM dyes. Overlap between absorption of PM546 and fluorescence of PM597 (PM567) is negligible. The triplet yield of PM597 is not negligible [16]. The longer triplet state lifetime can make energy transfer possible. In order to evaluate the Dexter triplet-triplet energy transfer mechanism (2), DFT calculations were performed to determine S_0 and T_1 energies. Calculated total energies for the S_0 and T_1 states and the relative energies of the T_1 state are listed in Table 1. The T_1 energy of PM567 is in good agreement with the experimentally obtained value of $37.9 \text{ kcal mol}^{-1}$ [17]. The T_1 energy of PM546 is higher than those of PM567 and 597. Therefore, the triplet-triplet energy transfer is not a possible path. Since PM546 possesses a relatively high fluorescence yield in acetonitrile $\Phi = 0.93-0.95$ [16,18] and deoxygenated PM597 exhibited accelerated photodegradation upon

PM546 addition, PM546 sensitized singlet oxygen generation will be a minor path for PM dye degradation. Further validation of this was stable PM546 absorbance readings following the prolonged 532 nm irradiation of a 2.5×10^{-5} M PM546 acetonitrile solution. On the basis of the fluorescence quenching experiment, electron transfer may occur from the excited state of PM597 to the ground state of PM546. The predicted standard free energy changes (ΔG°) are displayed in Table 2. The ΔG° values were estimated using the Rehm-Weller equation

$$\Delta G^\circ = E(D/D^+) - E(A/A^-) - E_{00} - e^2 / \epsilon r_{DA} \quad (9)$$

where $E(D/D^+)$ and $E(A/A^-)$ are the half-wave oxidation and reduction potential for the donor and acceptor, respectively, E_{00} is the excitation energy, e is the electronic charge, ϵ is the dielectric constant of the solvent, and r_{DA} is the separation between the donor and the acceptor. The r_{DA} is equated to the sum of the radii of the donor and acceptor which were calculated at the B3LYP/6-31G(d) level. The free energy changes were exoergic. The probability of electron transfer is dependent upon the orbital overlap between donor and acceptor. The LUMO orbital of PM dyes is mainly delocalized in the pyrromethene difluoroborate framework with π character. The overlap of orbitals may be effective due to similar family structures, which results in efficient electron transfer,



(D: PM567 or PM597)

followed by [10]



In nonpolar *n*-hexane, solvent stabilization of the ion pair is weaker resulting in a shift of the equilibrium in Eq. (10) towards reactants. The failure to form the ion-pair leads to deactivation of this photodegradation mechanism.

3.3. Phosphorescence Quenching by PM546

The observed decrease in PM567 and PM597 photostability upon PM546 addition is in marked contrast to the reported photostability enhancement upon C540 addition [8]. In the present experiment accelerated photodegradation predominates in the competition between enhanced dye photostability and accelerated dye photodegradation upon PM546 addition. An additive's ability to enhance PM dye photostability is attributed to singlet oxygen quenching [1,6,7]. The PM546 singlet oxygen quenching rate constant was determined by recording the 1270 nm phosphorescence decay profiles of an irradiated $5.6 \times 10^{-5} \text{ mol dm}^{-3}$ rose bengal/acetonitrile solution with varying PM546 concentration. The phosphorescence temporal decay profiles are shown in Fig. 8 with fitting curves by an exponential function $c_0 + c_1 \exp(-c_2 t)$ via weighted linear regression. Increasing phosphorescence decay rates are observed for increasing PM546 concentration consistent with $^1\text{O}_2$ quenching by PM546. A $^1\text{O}_2$ quenching rate constant of $3.86 \pm 0.18 (2\sigma) \times 10^7 \text{ dm}^3 \text{ mol}^{-1} \text{ s}^{-1}$ was obtained from the Stern-Volmer plot of the apparent quenching rate constants vs. PM546 concentration in Fig. 9. The obtained value is close to that reported for PM567 in benzene [17]. The observation of accelerated PM dye photodegradation upon PM546 addition despite the significant $^1\text{O}_2$ quenching rate constant, suggests faster kinetics for PM546 electron transfer (Eq. (10)) rather than PM546 $^1\text{O}_2$ quenching.

(Figs. 8, 9)

4. Conclusions

The PM567 and PM597 photostability dependence upon PM546 was investigated in solution by measuring absorption spectra following 532 nm laser irradiation. Photodegradation rates increased with increasing PM546 concentration. Fluorescence quenching of PM597 by PM546 was observed in acetonitrile. Electron transfer from the excited state of PM597 to the ground state of PM546 was considered as the mechanism responsible for the fluorescence quenching and the accelerated PM dye photodegradation. The singlet oxygen quenching rate constant of PM546 in acetonitrile was determined to be $3.86 \pm 0.18 (2\sigma) \times 10^7 \text{ dm}^3 \text{ mol}^{-1} \text{ s}^{-1}$. This suggests that in addition to the singlet oxygen concerned photodegradation mechanism, photoinduced electron transfer between the dye and the additive, which also acts as a singlet oxygen quencher, must be considered.

Acknowledgements

The authors are grateful to Prof. T. Fujii of Shinshu University for his encouragement throughout this work.

References

- [1] M.D. Rahn, T.A. King, *Appl. Opt.* 34 (1995) 8260.
- [2] M. Canva, P. Georges, J.-F. Perelgritz, A. Brum, F. Chaput. J.-P. Boilot, *Appl. Opt.* 34 (1995) 428.
- [3] W.N. Sisk, N. Ono, T. Yano, M. Wada, *Dyes and Pigments* 55 (2002) 143.
- [4] G. Qian, Y. Yang, Z. Wang, C. Yang, Z. Yang, M. Wang, *Chem. Phys. Lett.* 368 (2003) 555.
- [5] W.N. Sisk, W. Sanders, *J. Photochem. Photobiol. A: Chem.* 167 (2004) 185.

- [6] M.D. Rahn, T.A. King, A.A. Gorman, I. Hamblett, *Appl. Opt.* 36 (1997) 5862.
- [7] M.S. Mackey, W.N. Sisk, *Dyes and Pigments* 51 (2001) 79.
- [8] M. Ahmad, T.A. King, D.-K. Ko, B.H. Cha, J. Lee, *Opt. Laser Tech.* 34 (2002) 445.
- [9] G. Jones II, S. Kumar, O. Klueva, D. Pacheco, *J. Phys. Chem. A* 107 (2003) 8429.
- [10] M.J. Frisch, G.W. Trucks, H.B. Schlegel, G.E. Scuseria, M.A. Robb, J.R. Cheeseman, J.A. Montgomery, Jr., T. Vreven, K.N. Kudin, J.C. Burant, J.M. Millam, S.S. Iyengar, J. Tomasi, V. Barone, B. Mennucci, M. Cossi, G. Scalmani, N. Rega, G.A. Petersson, H. Nakatsuji, M. Hada, M. Ehara, K. Toyota, R. Fukuda, J. Hasegawa, M. Ishida, T. Nakajima, Y. Honda, O. Kitao, H. Nakai, M. Klene, X. Li, J.E. Knox, H.P. Hratchian, J.B. Cross, C. Adamo, J. Jaramillo, R. Gomperts, R.E. Stratmann, O. Yazyev, A.J. Austin, R. Cammi, C. Pomelli, J.W. Ochterski, P.Y. Ayala, K. Morokuma, G.A. Voth, P. Salvador, J.J. Dannenberg, V.G. Zakrzewski, S. Dapprich, A.D. Daniels, M.C. Strain, O. Farkas, D.K. Malick, A.D. Rabuck, K. Raghavachari, J.B. Foresman, J.V. Ortiz, Q. Cui, A.G. Baboul, S. Clifford, J. Cioslowski, B.B. Stefanov, G. Liu, A. Liashenko, P. Piskorz, I. Komaromi, R.L. Martin, D.J. Fox, T. Keith, M.A. Al-Laham, C.Y. Peng, A. Nanayakkara, M. Challacombe, P.M.W. Gill, B. Johnson, W. Chen, M.W. Wong, C. Gonzalez, J.A. Pople, *Gaussian 03, Revision B.03*, Gaussian, Inc., Pittsburgh PA, 2003.
- [11] M. Ahmad, T.A. King, D.-K. Ko, B.H. Cha, J. Lee, *Opt. Comm.* 203 (2002) 327.
- [12] K. Kang, W.N. Sisk, M. Yasin, F. Farahi, *J. Photochem. Photobiol. A: Chem.* 121 (1999) 133.
- [13] R.D. Scurlock, P. R. Ogilby, *J. Photochem. Photobiol. A: Chem.* 72 (1993) 1.
- [14] M.A.J. Rodgers, *J. Am. Chem. Soc.* 105 (1983) 6201.
- [15] J.B. Prieto, F.L. Arbeloa, V.M. Martínez, T.L. Arbeloa, I.L. Arbeloa, *J. Phys. Chem. A* 108 (2004) 5503.
- [16] R.Y. Lai, A.J. Bard, *J. Phys. Chem. B* 107 (2003) 5036.

[17] A.A. Gorman, I. Hamblett, T.A. King, M.D. Rahn, J. Photochem. Photobiol. A: Chem. 130 (2000) 127.

[18] F.L. Arbeloa, T.L. Arbeloa, I.L. Arbeloa, J. Photochem. Photobiol. A: Chem. 121 (1999) 177.

Figure Captions

Fig. 1 Changes in the absorption spectra of 1×10^{-5} mol dm⁻³ PM597 acetonitrile solution as a function of laser pulses.

Fig. 2 Photodegradation of 1×10^{-5} mol dm⁻³ pyrromethene dye solutions, where A/A_0 designates the absorbance maximum normalized to the absorbance maximum at 0 pulses. (Δ) PM597 in *n*-hexane, (\circ) PM567 in acetonitrile, (\square) PM597 in acetonitrile.

Fig. 3 Least-Squares fit of PM-597 concentration vs. number of pulses (t) to Eq. 7. (\circ) *n*-hexane solution and (\square) acetonitrile solution. Solid lines show the linear fits. Note: initial pulses are fitted for acetonitrile solutions.

Fig. 4 Photodegradation of mixtures of 1.0×10^{-5} mol dm⁻³ PM (567 or 597) and 2.5×10^{-5} mol dm⁻³ PM546.

(a) Absorption spectra of acetonitrile solutions of 1.0×10^{-5} mol dm⁻³ PM567, 1.0×10^{-5} mol dm⁻³ PM597, 2.5×10^{-5} mol dm⁻³ PM546.

(b) PM597 and PM567 normalized absorbance decay:

(Δ) PM597 absorbance of *n*-hexane solution of 1.0×10^{-5} mol dm⁻³ PM597

(\blacktriangledown) PM597 absorbance of *n*-hexane solution of 1.0×10^{-5} mol dm⁻³ PM597/ 2.5×10^{-5} mol dm⁻³ PM546

(\square) PM597 absorbance of acetonitrile solution of 1.0×10^{-5} mol dm⁻³ PM597

(■) PM597 absorbance of acetonitrile solution of 1.0×10^{-5} mol dm⁻³ PM597/ 2.5×10^{-5} mol dm⁻³ PM546

(○) PM567 absorbance of acetonitrile solution of 1.0×10^{-5} mol dm⁻³ PM567

(●) PM567 absorbance of acetonitrile solution of 1.0×10^{-5} mol dm⁻³ PM567/ 2.5×10^{-5} mol dm⁻³ PM546

(c) PM546 normalized absorbance decay:

(Δ) PM546 absorbance of *n*-hexane solution of 1.0×10^{-5} mol dm⁻³ PM597/ 2.5×10^{-5} mol dm⁻³ PM546

(□) PM546 absorbance of acetonitrile solution of 1.0×10^{-5} mol dm⁻³ PM597/ 2.5×10^{-5} mol dm⁻³ PM546

(○) PM46 absorbance of acetonitrile solution of 1.0×10^{-5} mol dm⁻³ PM567/ 2.5×10^{-5} mol dm⁻³ PM546

Fig. 5 Plots of absorbance ratios after 36,000 laser pulses vs. PM546 concentration. (○) PM597/PM546 in acetonitrile, (□) PM567/PM546 in acetonitrile.

Fig. 6 Oxygen dependence of PM597 photodegradation. (○) deoxygenated and (●) ambient air *n*-hexane solution, (Δ) deoxygenated and (▲) ambient air acetonitrile solution and (▼) ambient air PM597/PM546 (1:1) acetonitrile solution.

Fig. 7 Fluorescence quenching of PM597 by PM546 in acetonitrile. The PM546 concentrations are 0 (solid line), 1.8×10^{-3} (dotted line) and 2.7×10^{-3} (dashed line) mol dm⁻³.

Fig. 8 Time-resolved ¹O₂ phosphorescence following 532 irradiation of rose bengal/acetonitrile solution with varying PM546 concentration.

Fig. 9 Stern-Volmer plot of the apparent rate constant vs. PM546 concentration.

Table 1

Calculated total energies for the S_0 and T_1 states in hartrees and the relative energies of the T_1 state E_T in kcal mol⁻¹

| | HCTH/3-21G | | | B3LYP/3-21G(d) | | |
|-------|--------------|--------------|-------|----------------|--------------|-------|
| | S_0 | T_1 | E_T | S_0 | T_1 | E_T |
| PM546 | -873.1806645 | -873.1190955 | 38.61 | -873.2061878 | -873.1446925 | 38.59 |
| PM567 | -1029.617821 | -1029.557958 | 37.56 | -1029.616355 | -1029.556248 | 37.72 |
| PM597 | -1186.020021 | -1185.963281 | 35.60 | -1185.996168 | -1185.938160 | 36.40 |

Table 2

Photochemical and electrochemical properties of PM dyes.

| | $E(D/D^+) / V^a$ | $E(A/A^-) / V^a$ | E_{00} / eV | $\Delta G^\circ / eV$ |
|-------|------------------|------------------|---------------|-----------------------|
| PM546 | +1.22 | -1.18 | 2.52 | - |
| PM567 | +1.02 | -1.29 | 2.41 | -0.17 |
| PM597 | +1.01 | -1.24 | 2.38 | -0.15 |

^a Ref. [9].

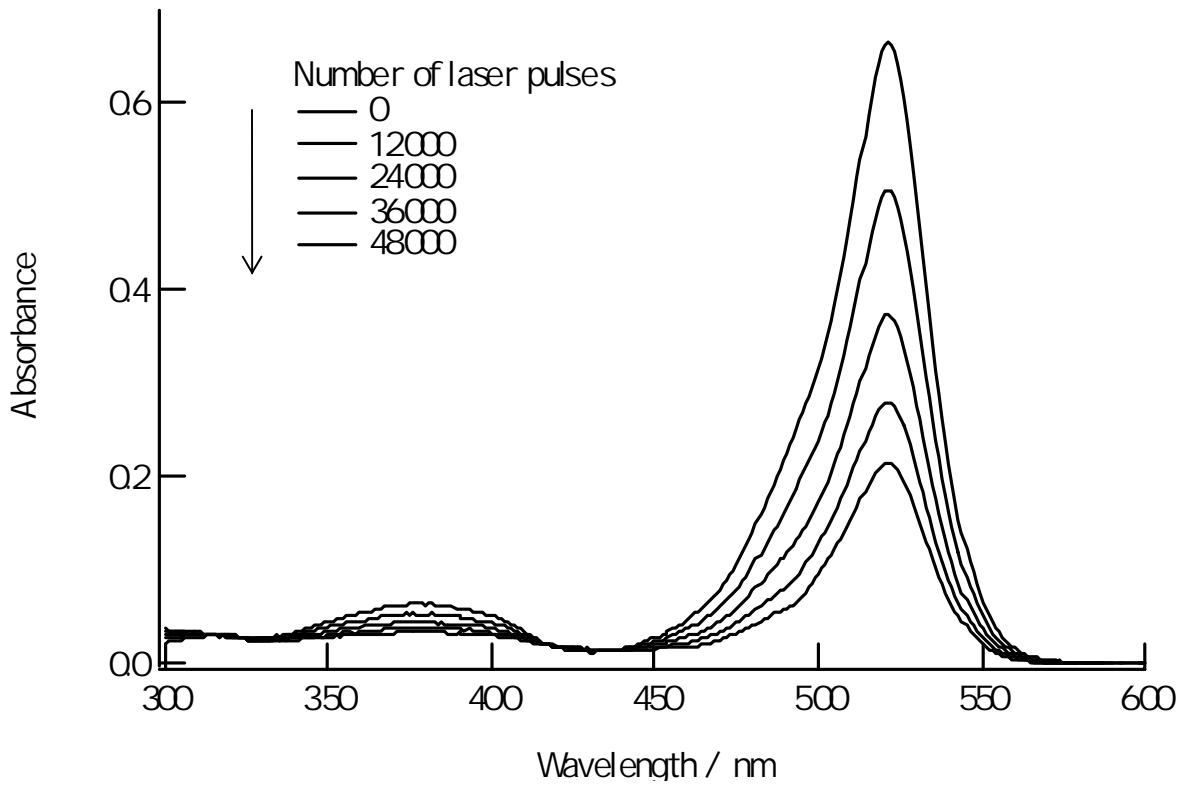


Fig. 1

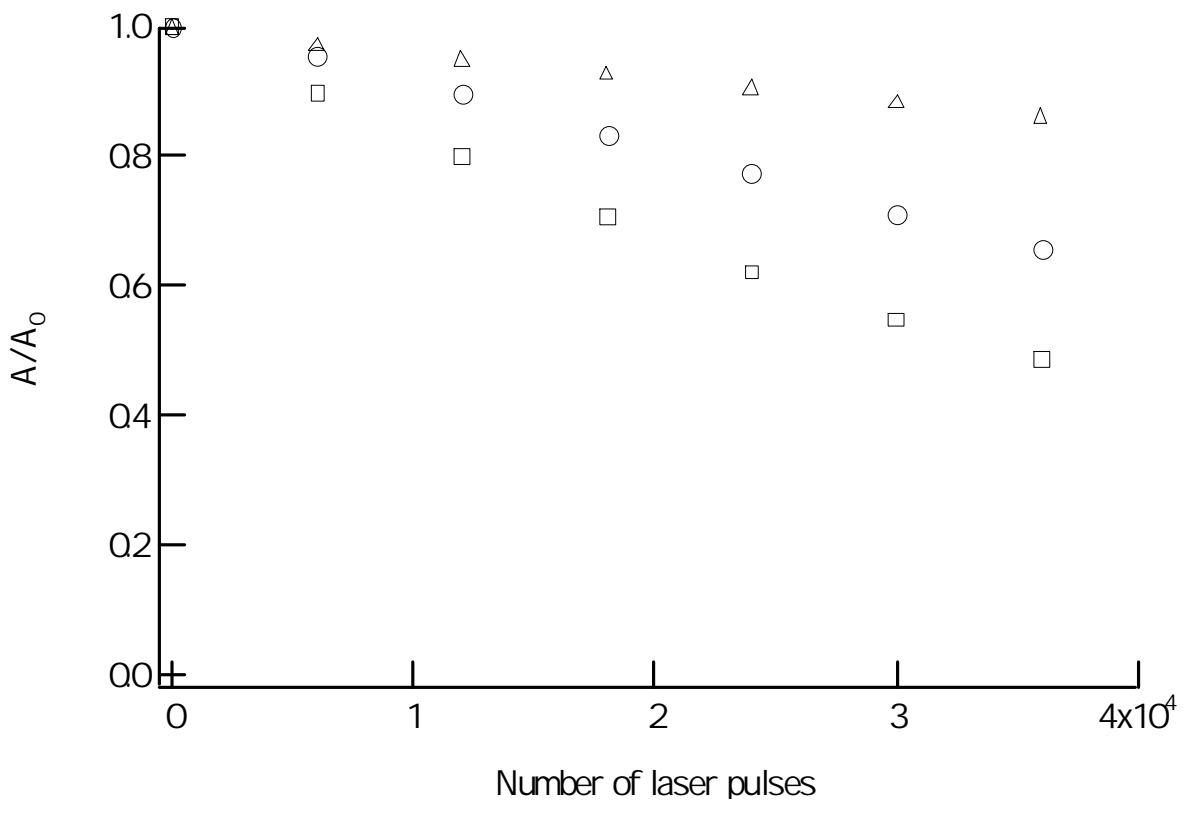


Fig. 2

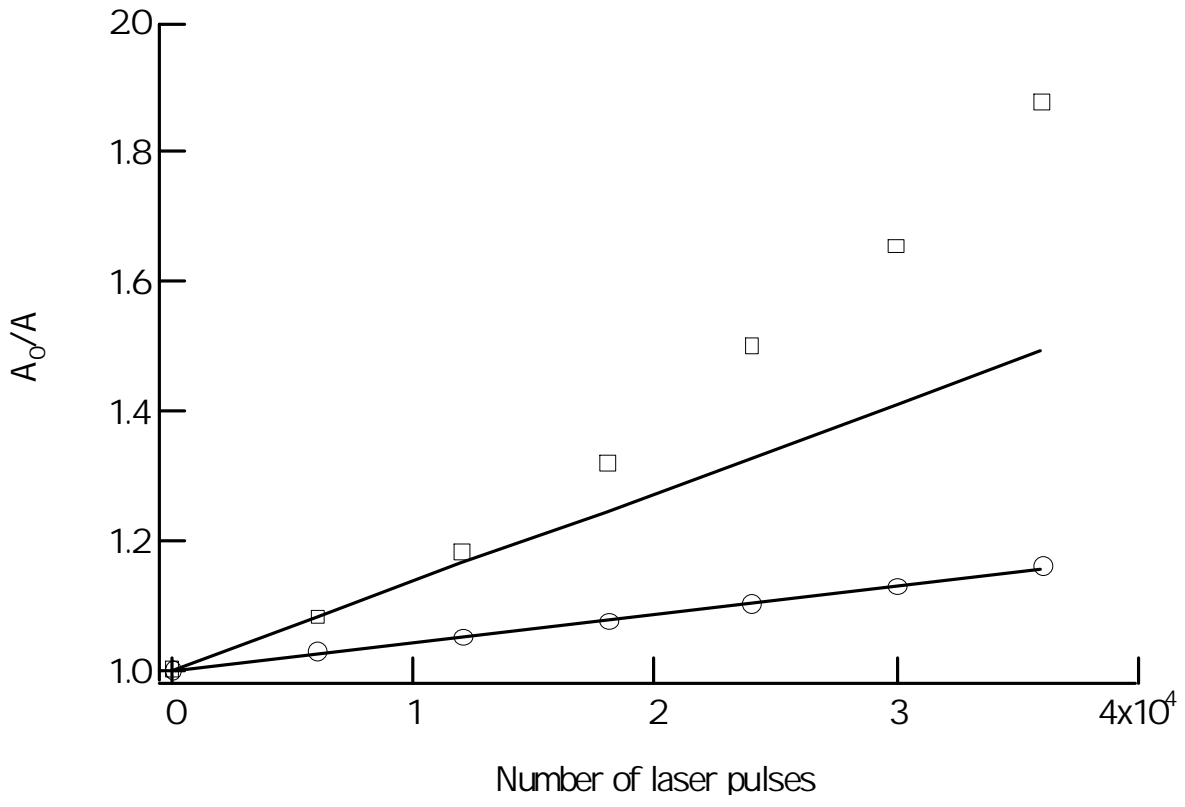


Fig. 3

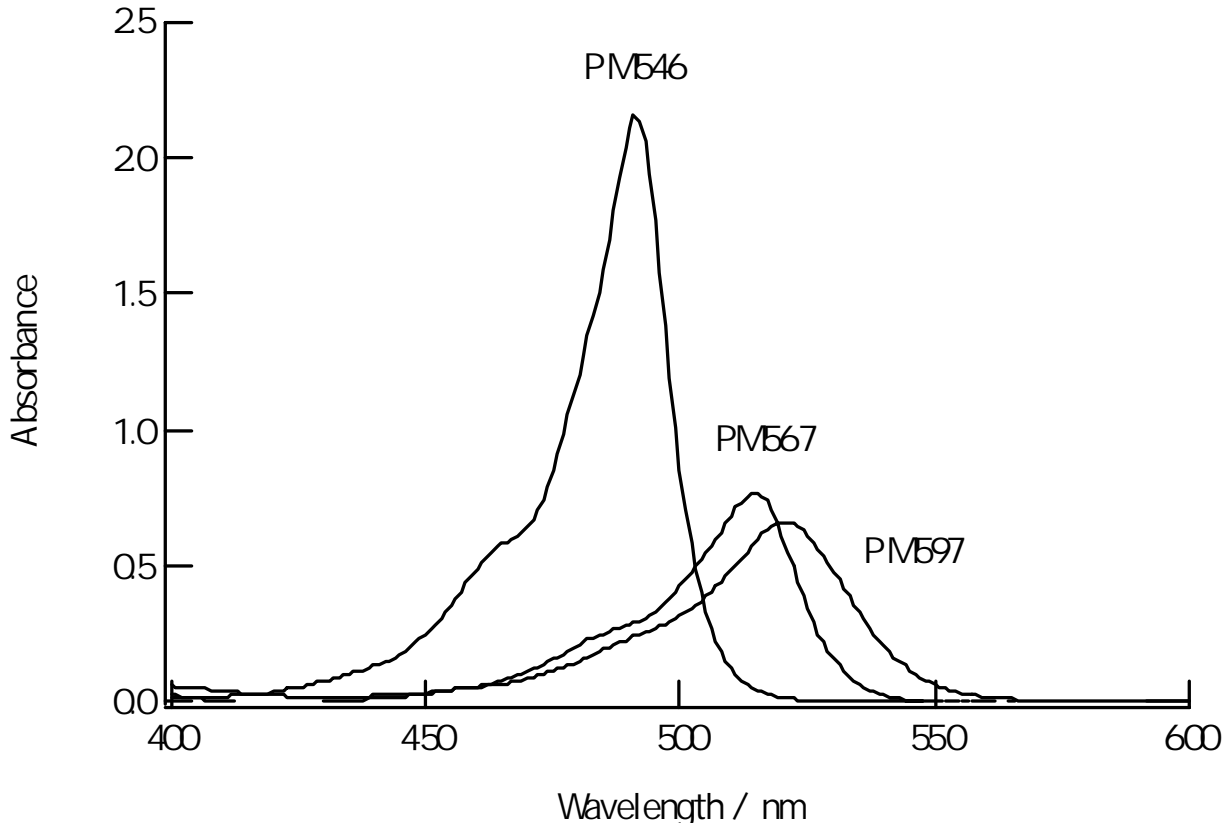


Fig. 4(a)

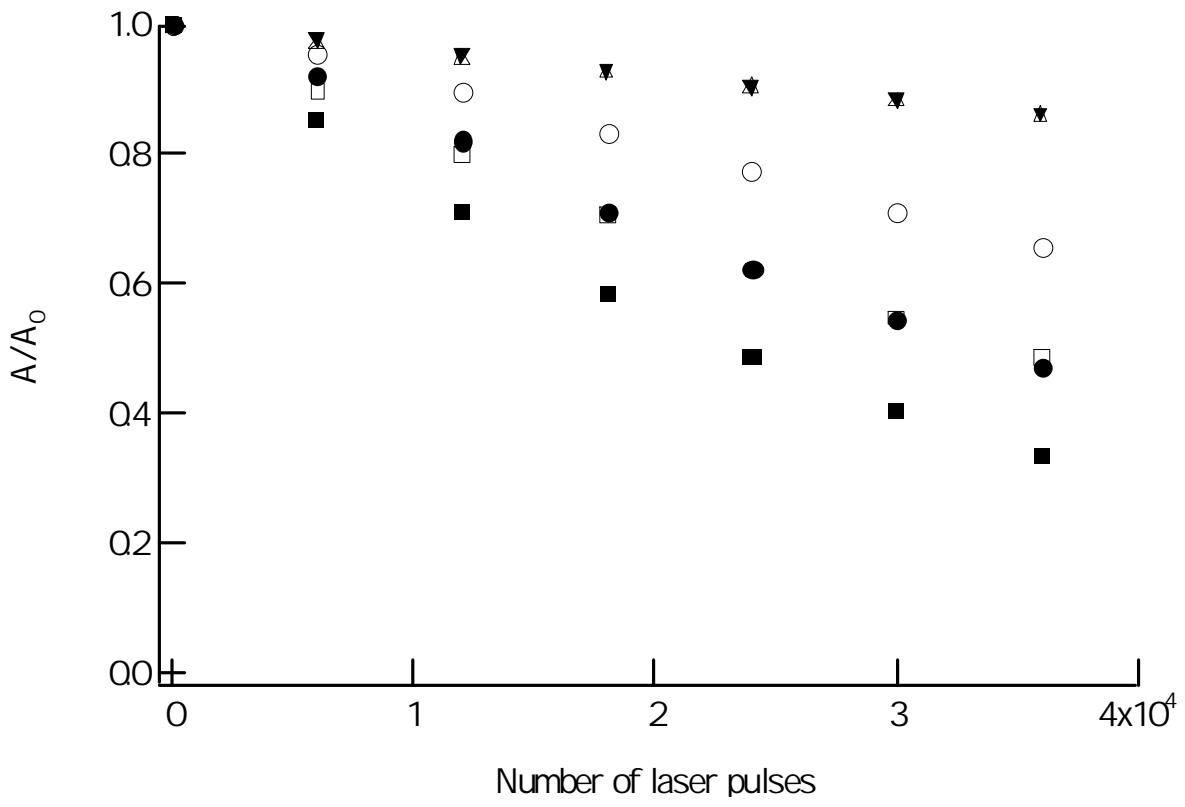


Fig. 4(b)

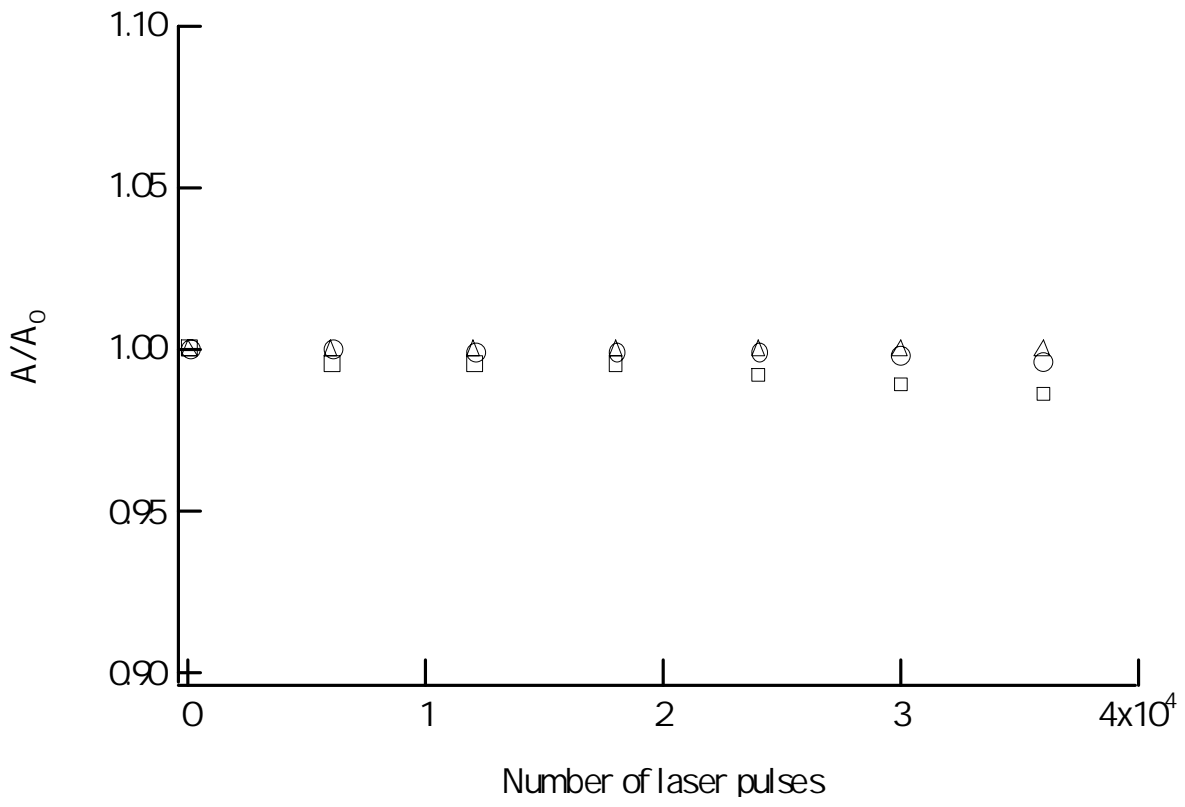


Fig. 4(c)

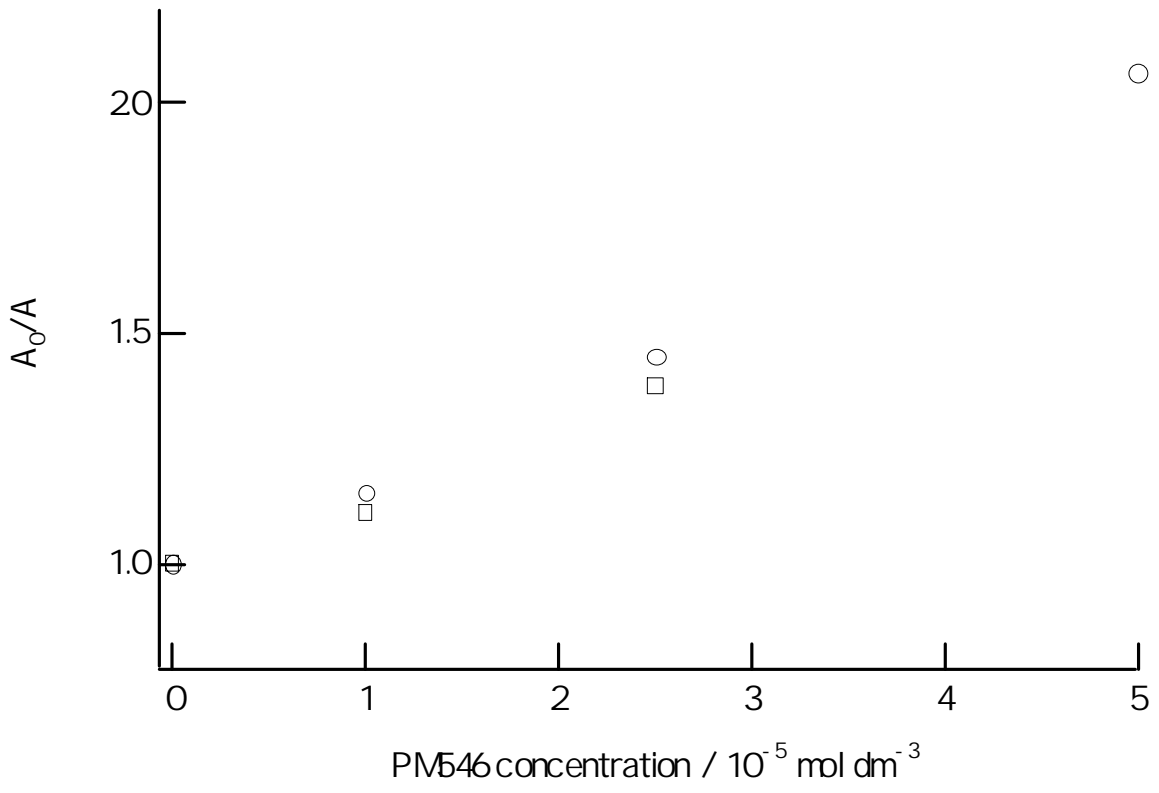


Fig. 5

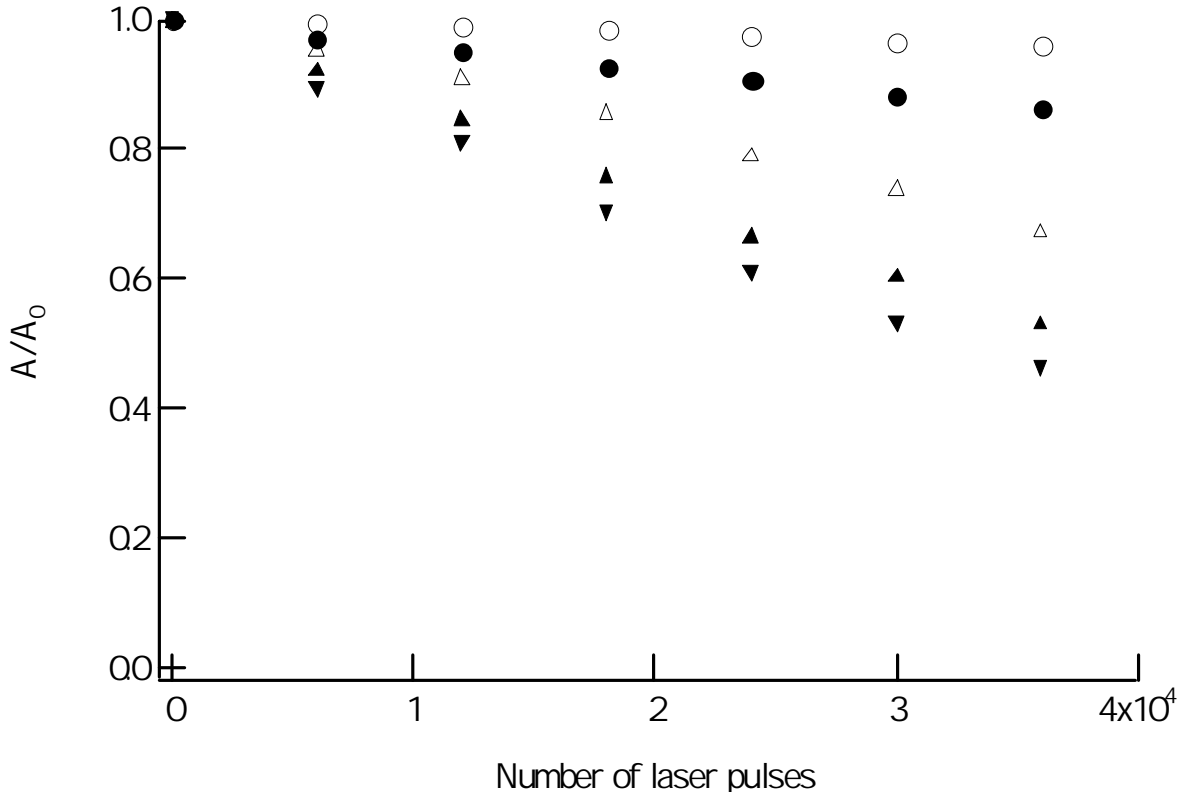


Fig. 6

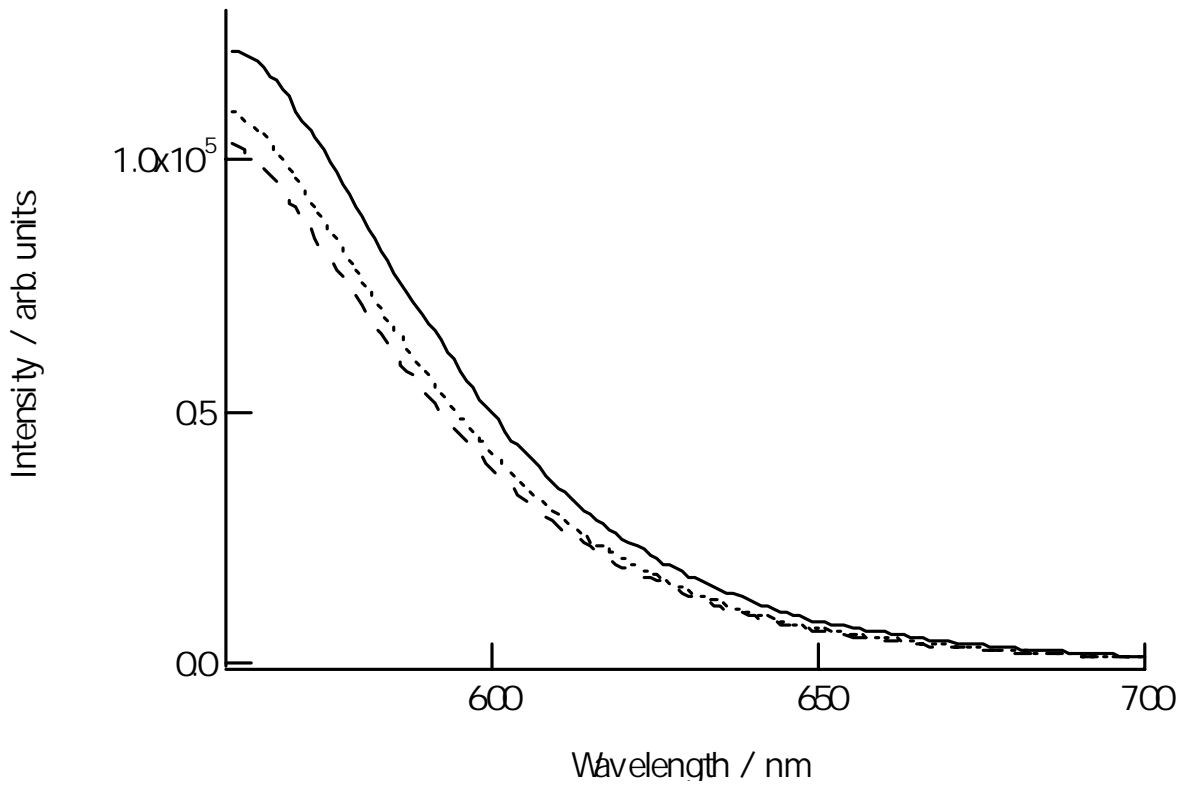


Fig. 7

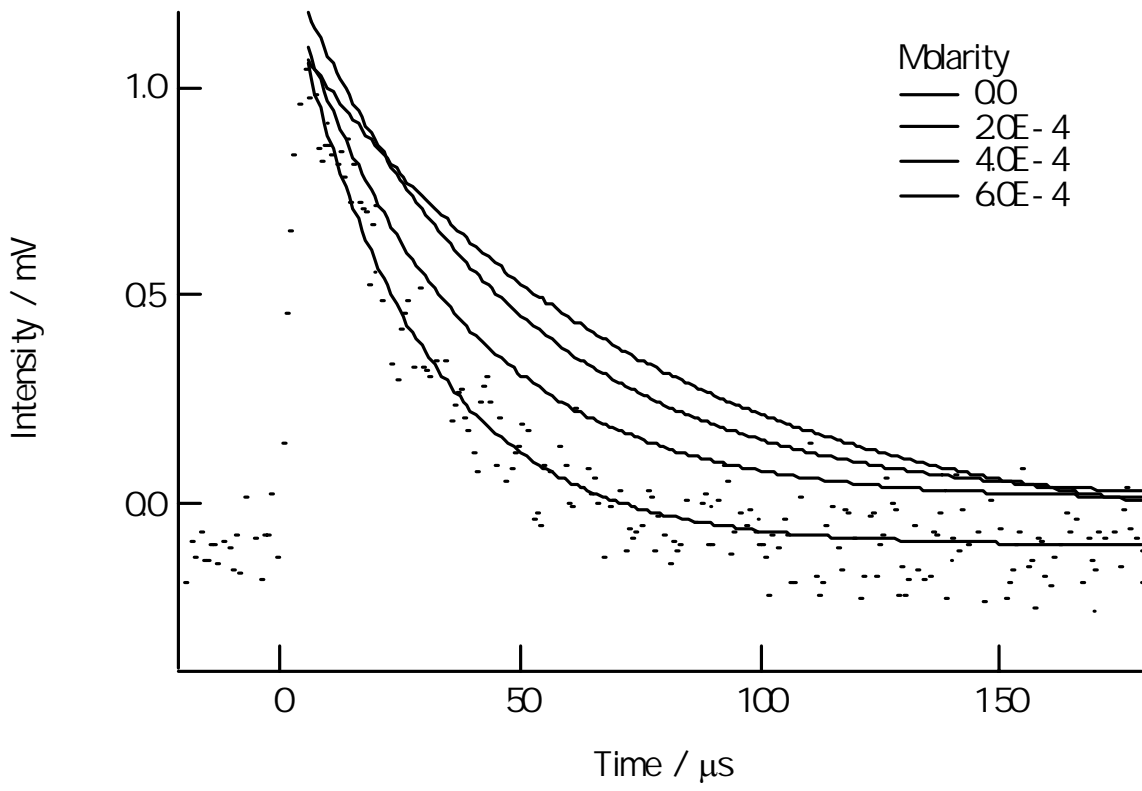


Fig. 8

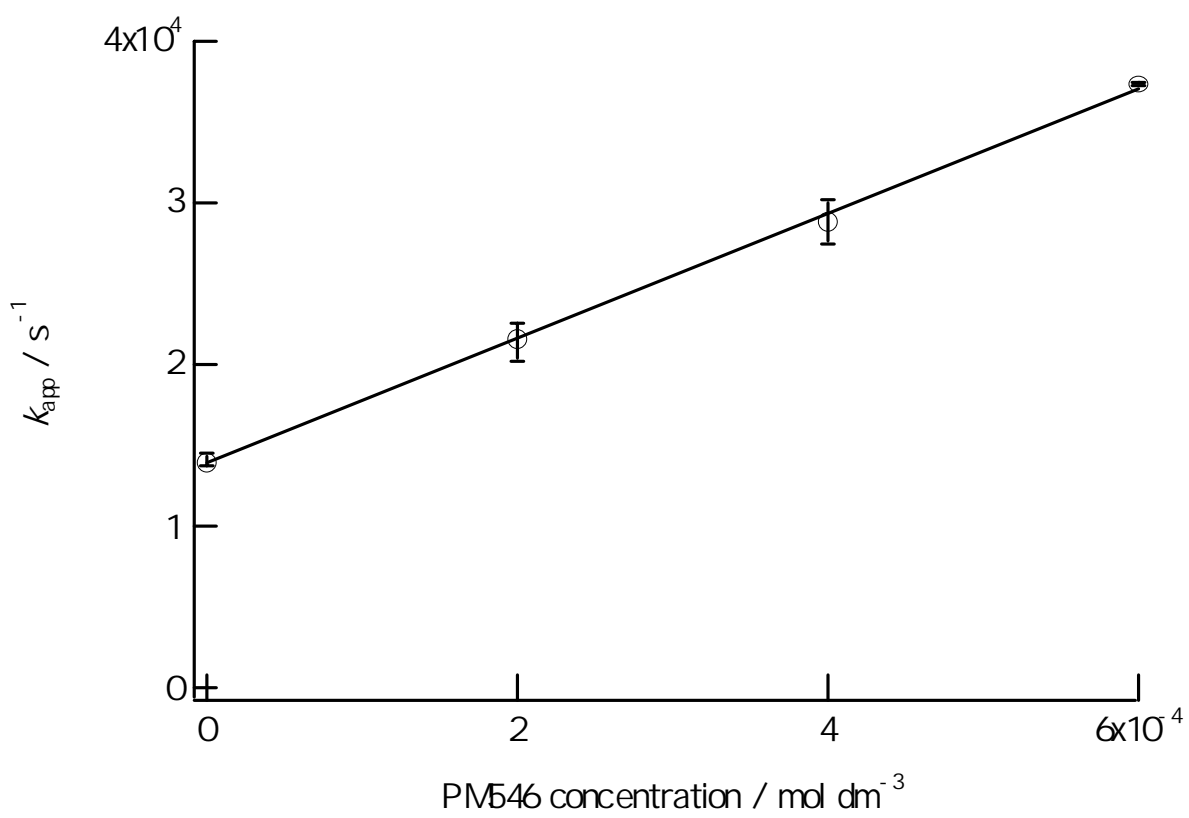


Fig. 9